The final publication is available at Springer via http://dx.doi.org/ 10.1007/s00216-014-8405-4

Analytical and Bioanalytical Chemistry, **February 2015, Volume 407, Issue 6, pp 1533-1543**

Isothermal circular strand displacement polymerization of DNA and microRNA in digital microfluidic devices

Maria Chiara Giuffrida[1], Laura Maria Zanoli[2], Roberta D'Agata[2], Alessia Finotti[3], Roberto Gambari[3], Giuseppe Spoto[1,2*]

[1] I.N.B.B. Consortium, Viale delle Medaglie D'Oro, 305, 00136 Roma, Italy

[2] Dipartimento di Scienze Chimiche, Università di Catania, Viale A. Doria 6, 95125, Catania, Italy

[3] Dipartimento di Scienze della Vita e Biotecnologie, Section of Biochemistry and Molecular Biology, University of Ferrara, Italy

*Corresponding author: spotog@unict.it; Tel.: +39-095-738-5141; Fax: +39-095-580138

Keywords:

Digital microfluidics, Nucleic acids amplification, microRNA, Isothermal amplification, circular strand displacement polymerization.

Abstract

Nucleic acid amplification is a key step in nucleic acid sequences detection assays. The use of digital microfluidic devices to miniaturize amplification protocols reduces the required sample volume and the analysis times and offers new possibilities for the process automation and integration in one single device. The recently introduced droplet polymerase chain reaction (PCR) amplification methods require repeated cycles of three or two temperature-dependent steps during the amplification of the nucleic acid target sequence. In contrast, low temperature isothermal amplification methods have no need for thermal cycling thus requiring simplified microfluidic device features. Here, the combined use of digital microfluidics and molecular beacon (MB)-assisted isothermal circular strand displacement polymerization (ICSDP) technique to detect microRNA-210 sequences is described. microRNA-210 has been described as the most consistently and predominantly upregulated hypoxia-inducible factor. The nM/pM detection capabilities of the method have been preliminarily tested by targeting single stranded DNA sequences from the genetically modified Roundup Ready soybean. The ability of the droplet ICSDP isothermal method to discriminate between full-matched, single mismatched and unrelated sequences has been also investigated. The detection of a range of nM/pM microRNA-210 solutions compartmentalized in nanoliter-sized droplets was performed to demonstrate the method capabilities for detecting as low as 10^{-18} moles of microRNA target sequences compartmentalized in 20 nL droplets. The method capability to operate with biological samples was tested by detecting microRNA-210 from transfected K562 cells.

Introduction

Digital microfluidics (also known as droplet microfluidics) has emerged as a key technology for DNA and RNA amplification and detection.[1] Compared with the macroscale, the microfluidic environment offers important advantages in biomolecular detection, such as reduced sample volumes required for the analysis, short analysis time, and potential for automation and integration.[2] Such advantages are particularly desirable in nucleic acid amplification and detection.[3]

The most renowned and currently widely used nucleic acid amplification technique exploits the polymerase chain reaction (PCR). The method is simple, sensitive and cost-effective. However, it is prone to sample contamination and suffers from biases in the template to product ratios of the amplified target sequences.[4] The method relies on thermal cycling in vitro to reach a maximum of twofold amplification in each cycle. The need for repeated heating and cooling steps represents an important limitation of the method, particularly when the full exploitation of advantages associated with the integration of nucleic acid amplification protocols in microfluidic-based devices is going to be achieved.[5,6] In order to overcome such a limitation, several alternative isothermal amplification methods have been developed.[7] These methods do not require thermal cycling, which greatly simplifies point-of-care diagnostics. In addition, they are often simpler and more tolerant to inhibitors present in real matrices than PCR. A number of different isothermal methods have been introduced over the last ten years, including nucleic acid sequence-based polymerization (NASBA), loop-mediated amplification (LAMP), helicase-dependent amplification (HDA), rolling circle amplification (RCA), recombinase polymerase amplification (RPA) and multiple displacement amplification (MDA).[2,7] Recently, the isothermal circular strand-displacement polymerization (ICSDP) has emerged as a new and promising method for nucleic acid amplification and detection.[8] The method belong to the molecular beacon (MB)-assisted isothermal methods group that is attracting even more interest for the inherent stability and selectivity in amplifying target sequences.[9],[10] In particular, ICSDP

relies on a hairpin fluorescence probe carrying a fluorophore (6-FAM) and a quencher (Black Hole Quencher 1, BHQ-1) moieties linked to the ends of the stem (Fig. 1). The hairpin loop sequence is designed in order to be complementary to the target sequence. A primer complementary to the stem region at 3'-end of the probe is also used. In the absence of the target, the hairpin probe is unable to anneal with the primer. Instead, the hairpin probe undergoes a conformational change leading to stems separation as a consequence of the probe-target hybridization (Fig. 1.I). Following this process, the primer anneals with the open stem (Fig. 1.II) and triggers a polymerization reaction in the presence of both DNA polymerase I (Exo^- Klenow Fragment) and dNTPs that causes the primer extension and target displacement (Fig. 1.III). The displaced target recognizes and hybridizes with another probe, triggering the next round of polymerization reaction. The hairpin conformational change results in the separation of the quencher from the fluorophore and in the generation of a fluorescent signal that linearly increases as the amplification reaction proceeds.

Micro RNAs (miR) are a group of small, non-coding RNAs that have emerged as a novel and rapidly expanding area of interest in clinical diagnostics.[11] They play important roles in almost every biological process, including cell fate determination, proliferation, and cell death.[12,13,14] In addition, miRs are implicated in cellular activities, such as immune response, insulin secretion, neurotransmitter synthesis, circadian rhythm, and viral replication.[15,16] miRs expression profiles have been linked to the diagnosis and prognosis of a variety of human cancers.[11] In addition, the presence of extracellular circulating miRs in biological fluids underlines the prominent role of miRs as biomarkers.[17] Unfortunately, miRs detection is challenging mostly because of their short length (19-23 nucleotides) and low concentration in biological fluids (nM-pM).[18] Even though a number of different approaches for the ultrasensitive detection of nucleic acid sequences have been recently described[19,20,21,22] the additional limitation represented by the length of the sequence introduce significant challenges to the development of new and efficient methods for miR detection.

Integration of PCR amplification in digital microfluidic devices has resulted in a dramatic expansion of possibilities in nucleic acid detection and quantification.[23] Digital PCR has been also applied for miR quantification.[24,25]

Possibilities offered by digital isothermal methods in DNA detection have been demonstrated with specific attention to RPA,[26] LAMP,[27] MDA,[28] RCA[29] and hyperbranched RCA amplification methods.[30] However, at the best of our knowledge, no demonstrations of digital isothermal detection of miRs have been provided so far.

In this work, the combined use of digital microfluidics and MB-assisted ICSDP amplification for the selective detection of has-miR-210-3p (**miR-210 FM**) in nanoliter droplets is presented. MicroRNA miR-210 is a key player associated with endothelial cell hypoxia,[31] differentiation and fetal hemoglobin production in erythroid cells.[32,33] Accordingly quantification of miR-210 is becoming a key step for diagnosis, prognosis and prediction of therapeutic response in several human pathological conditions, such as fetal hypoxia in-utero,[34] aortic stenosis[35] and renal[36], pancreatic[37] and prostate[38] cancers. Moreover, circulating serum levels of miR-210 were found to correlate with sensitivity to trastuzumab and tumor presence in breast cancer patients.[39]

Possibilities offered by droplet ICSDP in amplifying and detecting nucleic acid sequences were preliminarily investigated by detecting a Roundup Ready Soybean (**RRSoy FM**) related oligonucleotide sequence.[40] Performances of droplet ICSDP in discriminating between full-matched and single mismatched sequences were also demonstrated.

Materials and methods

Chemicals and reagents

Experiments were carried out by using ultra-pure nuclease free water (Milli-Q Element, Millipore). 3M™ Fluorinert™ Electronic Liquid FC-3283 was used as the carrier (3M). 1H,1H,2H,2H-perfluoro-1-octanol (PFO) 97%, tris-(hydroxymethyl)-aminomethane (TRIS), deoxynucleotides (dNTPs), dimethylsulfoxide (DMSO), dithiothreitol (DTT) and $MgCl_2$ were

purchased from Sigma-Aldrich. RNaseOUT™ Recombinant Ribonuclease Inhibitor was purchased from Invitrogen™.

MiR-210, RR-soybean related oligonucleotides, primers and molecular beacons (Table 1) were purchased from Thermo Fisher Scientific. Klenow Fragment (3´→ 5´ exo-) was purchased from MedClone s.r.l.

Nucleic acid sequences folding and hybridization predictions were performed by using Mfold web server.

Fabrication of microfluidic devices

Microfluidic devices were fabricated in PDMS (poly-dimethylsiloxane) through the established replica molding method. PDMS channels were created through the replication from masters in polyvinyl chloride with depth of 80 µm and width of 300-400 µm as elsewhere described.[41] Replicas were formed from a 1:10 mixture of PDMS curing agent and prepolymer (Sylgard 184, Dow Corning, USA). The mixture was degassed under vacuum, poured onto the master in order to create a layer and then left polymerizing for 48 h at room temperature. The PDMS mold was peeled off from the master surface and repeatedly washed with ethanol and ultra-pure water, and dried before use. PEEK tubes (UpChurch Scientific, ID 0.508 mm; OD 0.774 mm) were inserted in holes drilled into the PDMS device as inlets and outlets. After 30 s of air plasma etching of the cleaned surfaces, carried out by using a Femto Diener Electronics plasma cleaner (40-kHz), the irreversible adhesion of PDMS molds on microscope cover glasses was obtained. After the air plasma etching, treated surfaces were quickly placed in contact with each other and the new device placed at 60 °C for 30 min. Microfluidic devices were used after at least 24 h from their fabrication in order to allow the PDMS hydrophobic surface to be recovered after the plasma treatment to facilitate the interaction of water-in-oil droplets produced in microfluidic devices.

An example of microfluidic devices used for the experiments is shown in Figure 2. Flow rates of the buffer (inlets 2 and 3) and ICSDP mix (MB, dNTPs and primer in the buffer. Inlet 1) solutions were kept at 0.2 μL min^{-1} while the flow rate of the carrier was 1 μL min^{-1}.

Equipment and procedures for droplet ICSDP

Two Harvard 33 Twin syringe pumps (Harvard Apparatus) were employed to handle syringes (Hamilton microsyringe model 1750 volume 500μL and Hamilton microsyringe model 1725 volume 250μL) used to control liquids flow in the microfluidic device. Pharmed BPT tubing (ID=0.25 mm, Cole Parmer) were used to connect syringes to microfluidic device inlets. 1 μL of target sample and Klenow Fragment exo- in buffer solutions were injected in the device through inlet 4 and inlet 5, respectively by using a 1 μL syringe (Hamilton Microliter model 7101). Inlets were clamped to allow a proper loading of solutions. Sample loading was managed differently for miR-210 detection. In this case, 200 nL of differently concentrated miR-210 FM or miR-210 CTR solutions were dispensed by using an automated 5 μL syringe (eVOL® XR automated syringe). In particular, a specific syringe dispensing method was designed in order to introduce 200 nL of differently concentrated sample and control solutions so as to be preceded and followed by 200 nL of buffer solution used for fluorescence signal reference into the microfluidic devices. To prevent any sample concentration alteration caused by diffusion at the interface between miscible phases, 200 nL of the immiscible carrier was introduced before and after each aqueous fraction. The sequence of the aqueous and immiscible fractions was closed with 500 nL of the immiscible carrier.

Experiments were carried out at 37°C. A home-made temperature control system consisting of a silicon heater (12 V; 1.25 W), a platinum sensing resistor (Pt 1000), a toroidal transformer (115-230 Vac Primary, 30VA and 50VA) (RS Components) and a microprocessor-based digital

electronic controller (THP 48, Technologic) was used to maintain the selected temperature (± 0.1 °C) during the experiments.

A Leica DM IL Fluo inverted microscope equipped with a Leica DFC 450C digital camera and a Lumen 200 (Prior Scientific Inc.) metal-halide lamp was used to observe droplet generation and to detect MB generated fluorescence. MB fluorescence was induced by filtered radiation produced with a Lumen 200 Prior scientific metal halide lamp. Image J 1.42 software was used for image analyses. The fluorescence intensity was quantified by considering the average brightness (pixel) from selected regions of interest (ROIs). The selected ROIs were chosen in order to include the area inside the selected droplet.

Referenced fluorescence intensity was obtained by subtracting the intensity of the fluorescence generated by MB in the presence of the complementary target from the intrinsic fluorescence of the amplification mix (blank). Control experiments were carried out by using unrelated miR and DNA sequences instead of the target sequence. Data shown have been obtained by averaging the referenced fluorescence intensity calculated from five or seven different droplets.

Human K562 cell cultures, transfection with pre-miR-210 and RT-qPCR

The human leukemia K562 cells were cultured in humidified atmosphere of 5% CO_2/air in RPMI 1640 medium (SIGMA, St. Louis, MO, USA) supplemented with 10% fetal bovine serum (FBS; Biowest, Nuaille, F), 50 U/ml penicillin, and 50 mg/ml streptomycin. Cell growth was studied by determining the cell number per ml with a Z2 Coulter Counter (Beckman Coulter, Fullerton, CA, USA). For transfection, K562 cells were seeded in 24-wells plates at a density of 100,000 cells/well in a final volume of 500 µl and transfected with pre-miR-210 (ID: PM10516, Ambion, Life Technologies, Carlsbad, CA, USA) at a final concentration of 270 nM, using 6 µl of cationic liposome Lipofectamine RNAi Max (Invitrogen, Life Technologies, Carlsbad, CA, USA). All transfection steps were done accordingly to the manufacturer's protocol. After two

days, cells were re-transfected employing the same procedure. Total RNA was extracted 96 hours after transfection using the TRIzol® Reagent (Invitrogen). For validation of miR-210 content, 0.3 μg of total RNA were employed to convert miRNA-210 to cDNA and to perform the quantitative PCR amplification using an iCycler IQ5® (Bio-Rad, Hercules, CA, USA). The TaqMan® MicroRNA Assay and TaqMan® Universal PCR Master Mix, no AmpErase® UNG (Applied Biosystems, Foster City, CA, USA) was used. Changes in mRNA expression levels were calculated after normalization to calibrator genes (U6 and Let-7c). For quantification, the results were also compared with those obtained using the mature miR-210 oligonucleotide RT-qPCR-amplified as external reference (IDT Integrated DNA Technologies, Leuven, Belgium). The quantification by standard RT-qPCR was based on an external calibration protocol.

Results and discussion

Experiments were carried out by using a 10:1 mixture of FC-3283 and PFO as the carrier fluid which was injected in the main channel of the microfluidic device (Fig. 2(a), Inlet 6). Continuous flow rates of both the carrier fluid as well as the aqueous solutions were adjusted in order to obtain a continuous and reproducible droplets generation at the T-junction of the device where the aqueous phase meet the immiscible carrier fluid.

Droplet formation in a multiphase flow can be characterized by referring to the capillary number (*Ca*) defined as $Ca = \eta\nu/\gamma$, where η and ν are the viscosity (kg m^{-1} s^{-1}) and the velocity (m s^{-1}) of the continuous phase, respectively, and γ is the surface tension (kg s^{-2}) between the dispersed aqueous phase and the immiscible carrier fluid. Different *Ca* values result in different regimes of behavior of the multiphase flow. In particular, low *Ca* values produce a fast droplet separation from the T-junction. In this case, the process is dominated by the pressure drop across the droplet and droplets are produced with a reproducible frequency and distance between adjacent droplets.[42] It is for these reasons that experimental conditions were optimized so as to operate at

$Ca = 7.9 \times 10^{-5}$. Under similar experimental conditions about 20 nL in volume droplets were produced with low frequency (0.3 Hz) (Fig. 2(b)). Microfluidic devices were designed in order to introduce a time gap of 28 minutes between the droplet generation and the fluorescence detection useful to obtain the ICSDP amplification.

The mixing of the target and ICSDP mix solutions inside droplets was accelerated by chaotic advection while droplets were moving through winding channels in the device.

A typical experiment was carried out by detecting the fluorescence emitted from droplets where the isothermal amplification reaction was triggered by the interaction between the target sequence and MB.

The ICSDP method allows target hybridization, polymerization and target displacement processes to occur producing a fluorescence output useful to detect trace amount of the target sequence. In order to achieve a good fluorescence amplification it is important to accurately design the MB hairpin fluorescence probe sequence. MB stem sequence should ensure a proper stability of the stem structure so as to disfavor the stem sequence interaction with the primer in the absence of target thus preventing the polymerization reaction to be triggered by MB/primer interactions even in the absence of the target. On the other hand, sequences producing stem structures that are too stable would retain hairpin probe conformational change even in the presence of the target. MB stem structure used in this work consisted of 11-nt-long sequences (Table 1) while 8-nt and 7-nt-long primers were used for DNA and microRNA amplification, respectively. A shared-stem structure where one arm of the stem participates in either hairpin formation or target hybridization was designed in order to favor the stem hairpin structure opening in the presence of the target. In our case the shared sequence was constituted by six bases of the hairpin stem sequence close to 5'-end of MB which are complementary to the target.

Detection of Roundup Ready soybean DNA

Preliminary experiments aimed at investigating possibilities offered by droplet ICSDP were carried out by targeting the **RRSoy FM** sequence (Table 1) related to genetically modified Roundup Ready soybean. The **RRSoy CTR** sequence was used as the control. The real time detection of the fluorescence generated by ICSDP in the microfluidic device was performed by filling a channel of the device with the ICSDP reaction mix (**MB-RR** 0.36 μM, 8-mer primer 0.36 μM, Klenow fragment exo$^-$ 10U, dNTPs 720μM, DMSO 6%, DTT 1 mM, $MgCl_2$ 5 mM in 50 mM Tris-HCl buffer - pH 8.0) containing **RRSoy FM** target or **RRSoy CTR** control sequences (both 11 nM), respectively. Figure 3 shows the change of the referenced fluorescence intensity over time obtained when the **RRSoy FM** target was allowed to anneal with the **MB-RR** hairpin probe. The change of the detected fluorescence over time (linear within the investigated time interval - slope of 1.3×10^{-4} pixel s^{-1}), to be compared with the signal detected when the **RRSoy CTR** control was investigated, was caused by the conformational change of **MB-RR** probe triggered by the **RRSoy FM** hybridization.

Performances of droplet ICSDP in detecting nucleic acid sequences were investigated by adopting the microfluidics device shown in Fig. 2(a) under fully operative conditions. The detection of **RRSoy FM** and **RRSoy CTR** sequences was performed by using the already described ICSDP mix. In particular, in this case the three different arms of the microfluidic device defining the water fraction of the system were used to introduce solutions containing *i*) (Fig. 2; inlet 1) **MB-RR** 0.36 μM, **8-mer** primer 0.36 μM, dNTPs 720μM; *ii*) (Fig. 2(a); inlet 4) 1 μL of **RRSoy FM** or **RRSoy CTR** 300 pM in concentration and *iii*) (Fig. 2(a); inlet 5) 1 μL of 10U Klenow fragment exo$^-$, respectively. All solutions were in 50 mM Tris-HCl buffer (pH=8) added with DMSO 6%, DTT 1 mM, $MgCl_2$ 5 mM. The flow rate for each of the three channels was 0.2 μL min^{-1} while the carrier was introduced through inlet 6 with 1.0 μL min^{-1} flow rate. Droplets were formed at the water fraction/carrier junction. The three aqueous solutions were

compartmentalized and mixed in droplets thus producing a dilution of the target concentration by a factor of 3.

Fig. S1 of the Electronic Supplementary Material (ESM) shows the confidence interval of the mean at the 95% level of the referenced fluorescence signals detected when **RRSoy FM** 100 pM in concentration was detected. The detected fluorescence intensity was different (two-tailed t-test, level 95%, $\nu=8$, $p<0.0001$) than that emitted by unrelated RRSoy CTR 100 pM droplets. The ability to discriminate between full-matched, single mismatched and unrelated sequences represents an important feature of a nucleic acid detection technology. In order to evaluate droplet ICSDP performances in discriminating between the different interactions the referenced fluorescence detected with **165 pM RRSoy FM** solutions was compared to the signal detected when analyzing 165 pM samples carrying a single-base mismatch at the center (**mRRSoy C**) or more towards the end of the sequence (**mRRSoy 3'T** and **mRRSoy 5'C**) (Fig. 4). In this specific case, experiments were carried out at 40°C.

Sequences carrying a single-base mismatch generated fluorescence signals different (two-tailed t-test, level 95%, $\nu=8$, $p< 0.001$) than both the **RRSoy FM** full match and **RRSoy CTR** unrelated sequence, respectively. In addition, the position of the mismatch in the target sequence did not alter the method capability to discriminate between the full match and the control sequences. These results demonstrate the droplet ICSDP specificity in targeting complementary sequences by discriminating between full match sequences and sequences carrying a single-base mismatch even at hundreds pM concentrations.

Detection of miR-210

Mature miR-210 is formed in the cell cytoplasm as a consequence of DICER enzyme processing of the hairpin precursor miR (hsa-miR-210) sequence. The enzymatic process produces 22-nt long sequences able to mediate the translational inhibition of the targeted mRNA. The use of droplet ICSDP for **miR-210 FM** detection required to specifically design the molecular beacon

sequence (Table 1) to obtain the most efficient detection performances. In addition, the short **miR-210 FM** sequence to be targeted imposed the use of a 7-nt long primer. The shorter targeted sequence (22-nt vs. 26-nt) combined with the smaller primer (7-nt vs. 8-nt) used for the ICSDP process account for the reduced fluorescence intensity detected for **miR-210 FM** compared with **RRSoy FM**. Nevertheless, the real time detection of the fluorescence from static droplets comprising the ICSDP mix (**MB-miR** 0.31 μM, **7-mer** primer 0.31 μM, Klenow fragment exo$^-$ 10U, RNase OUTTM Recombinant Ribonuclease Inhibitor 40U, dNTPs 300 μM) and 12 nM **miR-210 FM** or **miR-210 CTR** sequences, respectively, demonstrated the efficacy of the method in discriminating between the **miR-210 FM** target and the unrelated **miR-210 CTR** control sequences (Fig. 5). The change over time of the fluorescence detected followed a saturating exponential model when the ICSDP process was applied for miR-210 detection.

Droplet ICSDP was then applied to the **miR-210 FM** detection by using the already described microfluidic device (Fig. 2). Also in this case the detection protocol was based on the sequential detection of fluorescence produced by droplets carrying blank solutions, **miR-210 FM** and **miR-210 CTR**. In order to fully demonstrate the possibilities offered by the digital microfluidic approach experiments were carried out by introducing 200 nL of the solution to be analyzed through the sample loading inlet (Fig. 2, inlet 4). In order to avoid any alteration in the concentration of the injected solutions caused by Taylor dispersion, the 200 nL aqueous solutions were compartmentalized in the device between 200 nL of the immiscible liquid used as the carrier in the microfluidic devices. Fluorescence from **miR-210 FM** and **miR-210 CTR** droplets formed at the water fraction/carrier junction was referenced to fluorescence from blank droplets so as to minimize instrumental fluctuations. The water fraction was constituted by solutions having the following composition: *i*) (Fig. 2(a); inlet 1) **MB-miR** 0.31 μM, **7-mer** primer 0.31 μM, dNTPs 300 μM, RNaseOUT 40U; *ii*) (Fig. 2(a); inlet 4) 200 nL of **miR-210 FM** or **miR-210 CTR** solutions followed by 200 nL of buffer and *iii*) (Fig. 2(a); inlet 5) 1 μL of Klenow fragment exo$^-$ 10U, respectively. Flow rate for aqueous solutions was 0.2 μL min^{-1}

while the carrier was introduced through inlet 6 with a 1.0 μL min^{-1} flow rate. Droplets 20 nL in volume were formed at the water fraction/carrier junction. Figure 6 shows the confidence interval of the mean at the 95% level of the referenced fluorescence signals detected when droplets carrying **miR-210 FM** with concentrations ranging from 165 pM to 4 nM solutions were detected. The detected signals show a saturation trend and a clear discrimination between target and unrelated sequences for the concentration range between 330 pM and 4 nM. For the lowest detected concentration (165 pM) no discrimination (level 95%; p=0.028) was obtained between the target and the control sequence.

Data shown demonstrate that the described isothermal method can be efficiently applied for the detection of 20 nL droplets carrying mature microRNAs sequences hundreds of pM in concentration. More specifically, fluorescence generated from one single droplet containing about 3.3 attomoles of **miR-210 FM** can be detected and discriminated from the unrelated **miR-210 CTR** sequence by combining droplet ICSDP with droplet microfluidics. The whole experiment can be performed by managing as low as 200 nL of the sample solution carrying as low as 6 x 10^7 mature miR-210 molecules.

Quantification of miR-210 from K562 cells

In order to achieve the proof-of-principle that droplet ICSDP is suitable for quantifying microRNAs from real biological matrices, miR-210 was analyzed in two RNA samples, one obtained from K562 cells after 96 hours after transfection with 270 nM pre-miR-210 (sample **270 96h**), the other obtained from control K562 cells cultured for 96 hours in the absence of treatments (**C1 96h**). miR samples were quantified for miR-210 content by RT-qPCR (Figure S2).Sample **270 96h** demonstrated to contain **18 nM** miR-210 (annealing temperature 60°C). The transfection of K562 cells with pre-miR-210, therefore, allows to obtain content higher more than 30-fold of mature miR-210. The detection experiments were carried out by introducing a sequence of (Fig. 2(a); inlet 4) 200nL of **270 96h,** buffer, **C1 96h** and buffer

solutions. To prevent any sample concentration alteration caused by diffusion at the interface between miscible phases, 400 nL of the immiscible carrier was introduced before and after each of the above mentioned solution. The water fraction of the microfluidic device was constituted by solutions having the following composition: **MB-miR** 0.31 μM, **7-mer** primer 0.31 μM, dNTPs 300 μM, RNaseOUT 40U (Fig. 2(a); inlet 1); 200 nL of **270 96h, C1 96h** of buffer solutions (Fig. 2(a); inlet 4); 1 μL of Klenow fragment exo$^-$ 10U (Fig. 2(a); inlet 5). Flow rate for aqueous solutions was 0.2 μL min^{-1} while the carrier (Fig. 2(a); inlet 6) was introduced with a 1.0 μL min^{-1} flow rate. The experiment was carried out at 37°C. Fluorescence from **270 96h** and **C1 96h** droplets was referenced to fluorescence from blank droplets. Fig. S2 (panel D) of the Electronic Supplementary Material (ESM) shows the confidence interval of the mean at the 95% level (two-tailed t-test, level 95%, ν=8, $p<0.0001$) of the referenced fluorescence signals detected when **270 96h** and **C1 96h** were injected into the microfluidic device. It is possible to clearly discriminate the fluorescence signal of the droplets carrying **270 96h** with respect to the control fluorescence signal. To allow the quantification of miR-210 in this biological sample a calibration curve was built [43,44,45,46] in the 0.33 nM and 1.66 nM miR-210 FM concentration range (Fig. 7). Also this experiment was carried out as already explained. The procedure allowed to calculate a concentration of miR-210 in the **270 96h** of 0.94± 0.14 nM (confidence interval of the mean at the 95% level), a concentration which is in the range of that obtained by RT-qPCR (18 nM) which is a standard procedure for microRNA quantification. In addition, the results obtained fully support the concept that different miR-210 levels can be detected. This is the major requirement in miRNA patterning in diagnostics. Despite the fact that additional experiments are necessary to extend the quantification of miR-210 to a larger number of samples, and to fully demonstrate differences existing between droplet ICSDP and RT-qPCR quantification, these data are the proofs-of-principle that droplet ICSDP can be employed to detect miRNAs in complex biological matrices.

Conclusions

When combined with digital microfluidics ICSDP offers a convenient environment for fast, simple and effective DNA and microRNA detection. In addition, droplet ICSDP isothermal procedure simplifies the integration of nucleic acids detection protocols in microfluidic devices.

We applied the new method for the detection of Roundup Ready soybean genetically modified sequence and miR-210. miR-210 was also detected in real biological matrices using RNA prepared from K562 cells samples transfected with pre-miRNA-210 and therefore producing high levels of mature miR-210. Potential offered by the method have been demonstrated by designing specific experiments using a total of 200 nL of solutions carrying a total of as low as 6 x 10^7 molecules. The method sensitivity, specificity and capabilities in discriminating between target and unrelated sequences as well as sequences carrying a single-base mismatch has been investigated. In addition, the method offers possibilities for detecting as low as 3.3 10^{-18} moles of microRNA target sequences compartmentalized in 20 nL droplets.

The new approach represents a promising tool for the development of simpler and more convenient lab-on-chip devices for miRNAs detection. Further experimental efforts are necessary to determine the detection limit of this technology in the quantification of miRNAs in clinically-relevant samples (for instance blood samples from cancer patients to detect circulating free miRNA as diagnostic/prognostic markers). Finally, further experiment are expected to generate a conversion table which will homogenize the data obtained with this strategy to those obtained with other approaches, such as the RT-qPCR, or droplet digital PCR, all of them based on very different concepts and strategies.

Acknowledgments

MIUR (PRIN 20093N774P), Ministry of Health, Italy (n. 098/GR-2009-1596647), COST Action TD1003-Bio-inspired nanotechnologies: from concepts to applications and the Italian

Association for Cancer Research (AIRC 13575: Peptide nucleic acids targeting oncomiR and tumor-suppressor miRNAs: cancer diagnosis and therapy) are acknowledged for partial financial support.

Table 1

Description	Sequence	Acronym	T_m
Target RR Soybean	5'AAGACCCTTCCTCTATATAAGGAAGTTTT3'	**RRSoy FM**	**54.9°C**
Control RR Soybean	5'TGGCTAGAGTAGAGTGAGCTAATCAATTT3'	**RRSoy CTR**	**56.1°C**
RR Soy inner mismatch	5'AAGACCCTTCCTCT**C**TATAAGGAAGTTTT3'(A→C)	**mRRSoy C**	**49.9°C**[a]
RR Soy outer mismatch 3'	5'AAGACCCTTCCTCTCTATAAG**T**AAGTTTT3'(G→T)	**mRRSoy 3'T**	**47.2°C**[a]
RR Soy outer mismatch 5'	5'AA**C**ACCCTTCCTCTCTATAAGGAAGTTTT3'(G→C)	**mRRSoy 5'C**	**47.5°C**[a]
Primer 8-mer	5'TCTTGACT3'	**8-mer**	**22°C**
Molecular Beacon RR Soy[b]	5'(6FAM) TCTTGACTTCCTTATATAGAGGAAGGG TCTTGGAAGTCAAGA (BHQ1)3'	**MB-RR**	**68.9°C**
Target hsa-miR-210-3p	5'CUGUGCGUGUGACAGCGGCUGA3'	**miR-210 FM**	**60.4°C**
Control miR-210	5'UCAUAGAGUACUAAUAUCAUCU3'	**miR-210 CTR**	**45.5°C**
Primer 7-mer	5'TCTTGTC3'	**7-mer**	**20°C**
Molecular Beacon miR-210[b]	5'(6-FAM) TCTTGTCAGCCGCTGTCACACGCA CAGGGCTGACAAGA (BHQ1) 3'	**MB-miR**	**80.8°C**

[a] Tm for mismatched sequences was calculate from IDT's Oligo Analyzer (Version 3.1)

[b] Complementary sequences of the hairpin stem are underlined. Red letters define the primer complementary sequence.

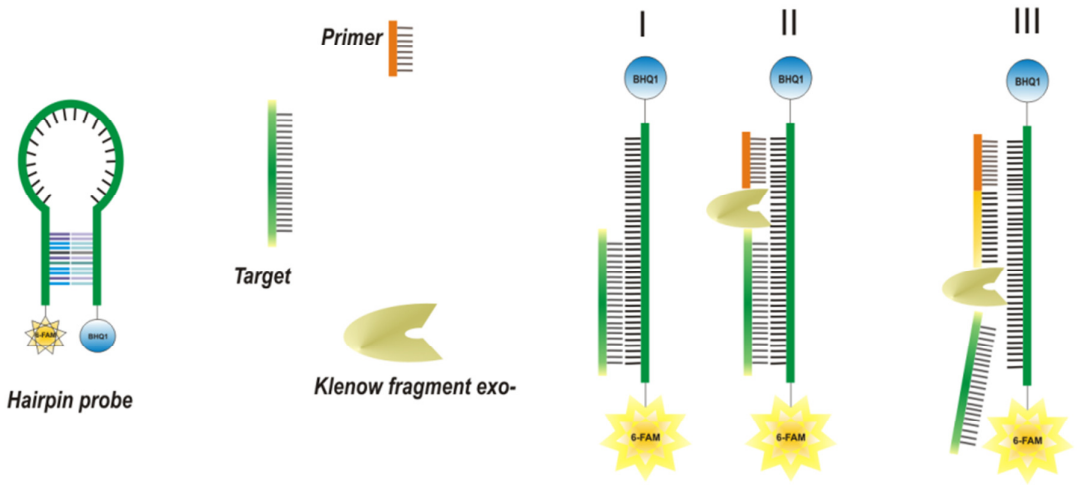

Figure 1: Schematic description of the isothermal circular strand displacement polymerization strategy.

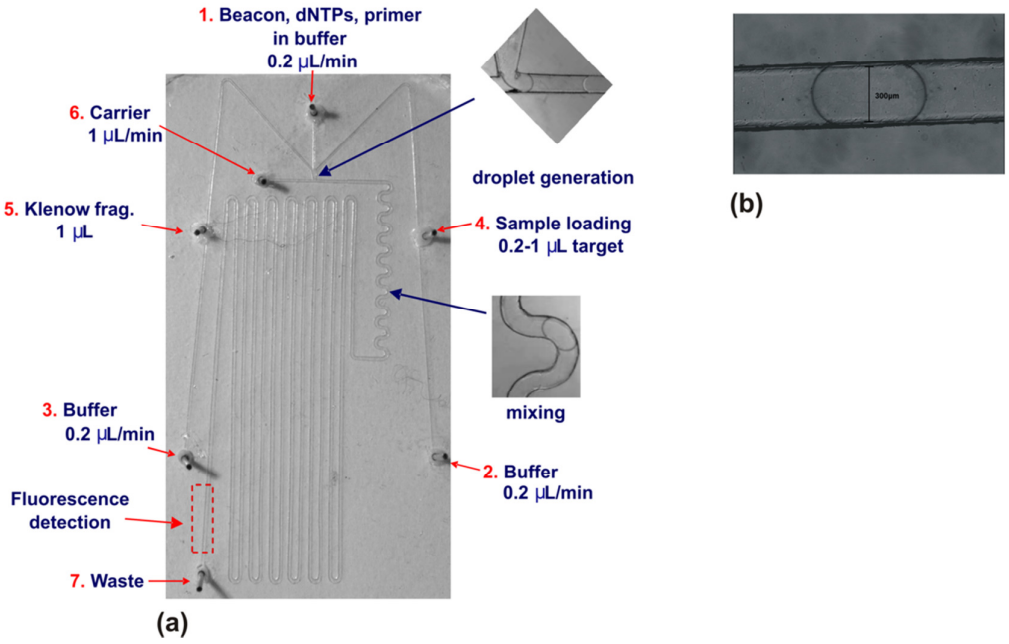

Figure 2: (a) Microfluidic device used for the droplet-based nucleic acid detection.
(b) Representative optical image of a droplet generated in the microfluidic device.

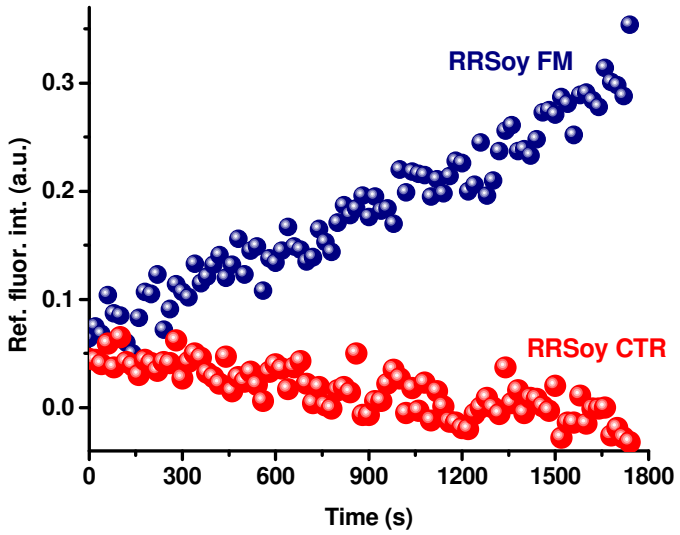

Figure 3 : Referenced fluorescence intensity versus time generated by ICSDP when 11 nM **RRSoy FM** and **RRSoy CTR** sequences were targeted. The experiment was carried out in the continuous microfluidic environment under static conditions.

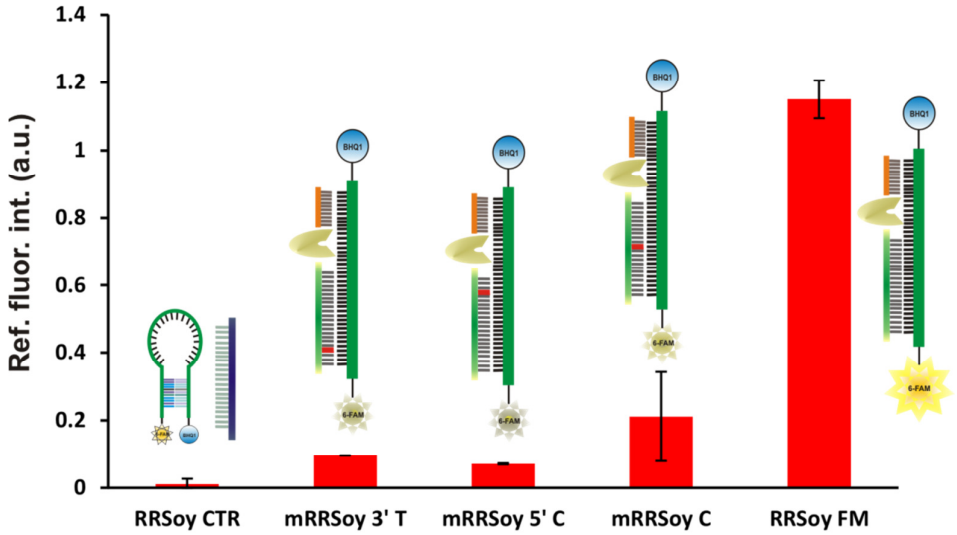

Figure 4: Average referenced fluorescence intensity (n=5) detected from **RRSoy FM** compared with those detected from **mRRSoy C**, **mRRSoy 5'T** and **mRRSoy 3'T** sequences carrying a single-base mismatch differently located in the sequence. The average referenced fluorescence intensity for the unrelated **RRSoy CTR** sequence is also shown. Detected solutions were 165 pM in concentration. The temperature during the experiment was maintained at 40°C. Error bars represent the confidence interval of the mean at the 95% level.

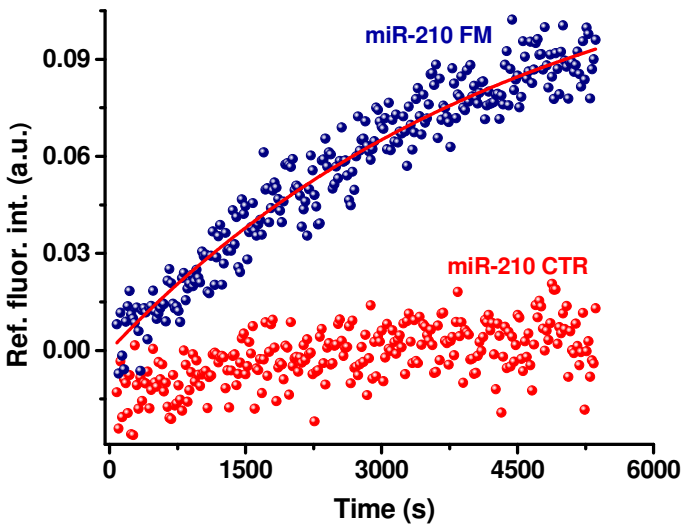

Figure 5: Referenced fluorescence intensity versus time generated by ICSDP when 12 nM **miR-210 FM** and **miR-210 CTR** sequences were targeted. The experiment was carried out in the continuous microfluidic environment under static conditions.

The non-linear regression for **miR-210 FM** (R^2= 0.939) was carried out by using a saturating exponential function ($y = a(1 - e^{-bx})$).

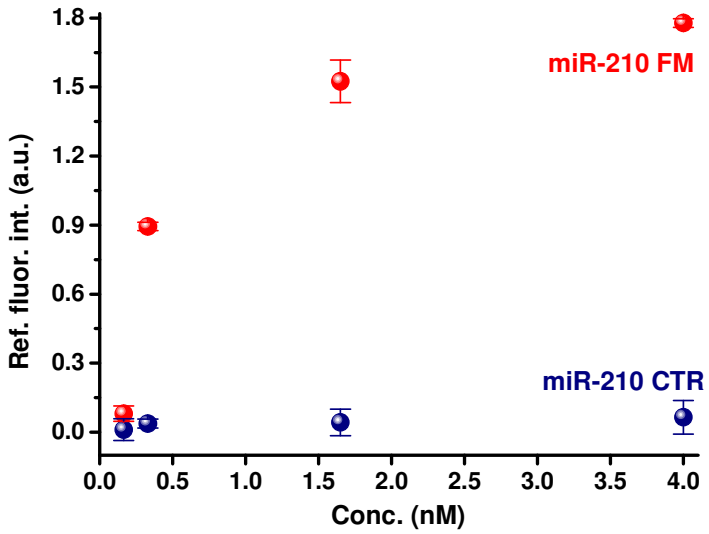

Figure 6: Average referenced fluorescence intensity produced after the droplet ICSDP detection of differently concentrated (range 165 pM- 4 nM) **miR-210 FM** solutions compared with the average referenced fluorescence intensity produced by the unrelated **miR-210 CTR** solutions having the same concentration (two-tailed t-test, level 95%, $\nu = 12$, $p<0.0001$). Error bars represent the confidence interval of the mean at the 95% level.

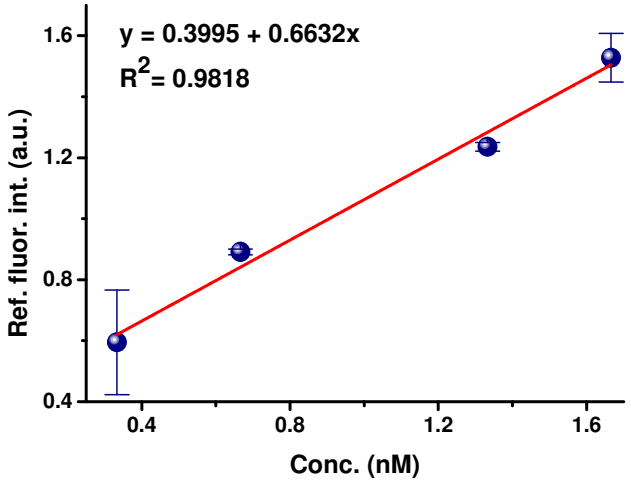

Figure 7: Calibration of the droplet ICSDP assay with concentrations of target miR-210 ranging between 0.33 nM and 1.66 nM. Error bars represent the confidence interval of the mean at the 95% level.

References

[1] Schneider T, Kreutz J, Chiu DT (2013) The potential impact of droplet microfluidics in Biology. Anal Chem 85:3476-3482.

[2] Zanoli LM, Spoto G (2013) Isothermal amplification methods for the detection of nucleic Acids in microfluidic devices. Biosensors 3:18-43.

[3] Spoto G, Corradini R (2012) Detection of non-amplified genomic DNA, Springer-Verlag.

[4] Pinto AJ, Raskin L (2012), PCR biases distort bacterial and archaeal community structure in pyrosequencing datasets. PlosOne 7: e43093.

[5] Craw P, Balachandran W (2012), Isothermal nucleic acid amplification technologies for point-of-care diagnostics: a critical review. Lab Chip 12:2469-2486.

[6] Asiello PJ, Baeumner AJ (2011), Miniaturized isothermal nucleic acid amplification, a review. Lab Chip 11:1420-1430.

[7] Kim J, Easley CJ (2011) Isothermal DNA amplification in bioanalysis: strategies and applications. Bioanalysis 3: 227-239.

[8] Guo Q, Yang X, Wang K, Tan W, Li W, Tang H, Li H (2009) Sensitive fluorescence detection of nucleic acids based on isothermal circular strand-displacement polymerization reaction. Nucl Acids Res 37(3), e20.

[9] Duan R, Zuo X, Wang S, Quan X, Chen D, Chen Z, Jiang L, Fan C, Xia F (2013) Lab in a Tube: Ultrasensitive detection of microRNAs at the single-cell level and in breast cancer patients using quadratic isothermal amplification. J Am Chem Soc 135(12):4604-4607.

[10] Duan R, Zuo X, Wang S, Quan X, Chen D, Chen Z, Jiang L, Fan C, Xia F (2014) Quadratic isothermal amplification for the detection of microRNA. Nat Protoc 9: 597-607.

[11] Nana-Sinkam SP, Croce CM (2013) Clinical applications for microRNAs in cancer. Clin Pharmacol Therap 93:98-104.

[12] Mendell JT, Olson EN (2012) MicroRNAs in stress signaling and human disease. Cell 148:1172-1187.

[13] Zampetaki A, Mayr M (2012) MicroRNAs in vascular and metabolic disease. Circ Res 110:508-522.

[14] Bartel DP (2009) MicroRNAs: target recognition and regulatory functions. Cell 136:215-33.

[15] Dong H, Lei J, Ding L, Wen Y, Ju H, Zhang X (2013) MicroRNA: function, detection, and bioanalysis. Chem Rev 113:6207-6233.

[16] Shivdasani RA (2006) MicroRNAs: regulators of gene expression and cell differentiation. Blood 108:3646-3653.

[17] Tzimagiorgis G, Michailidou EZ, Kritis A, Markopoulos AK, Kouidou S (2011) Recovering circulating extracellular or cell-free RNA from bodily fluids. Cancer Epidemiology 35: 580-589.

[18] Pritchard CC, Cheng HH, Tewari M(2012) MicroRNA profiling: approaches and considerations. Nat Rev Genet 13:358-369.

[19] D'Agata R, Breveglieri G, Zanoli LM, Borgatti M, Spoto G, Gambari R (2011) Direct detection of point mutations in non-amplified human genomic DNA. Anal Chem 83:8711-8717.

[20] D'Agata R, Spoto G (2013) Surface plasmon resonance imaging for nucleic acid detection. Anal Bioanal Chem 405:573-584.

[21] Zanoli LM, D'Agata R, Spoto G (2012) Functionalized gold nanoparticles for the ultrasensitive DNA detection. Anal Bioanal Chem 402:1759-1771.

[22] Spoto G, Minunni M (2012) Surface Plasmon Resonance Imaging: What Next?. J Phys Chem Lett 3: 2682-2691.

[23] Baker M (2012) Digital PCR hits its stride. Nat Methods 9:541-544.

[24] Hindson CM, Chevillet JR, Briggs HA, Gallichotte EN, Ruf IK, Hindson BJ, Vessella RL, Tewari M (2013) Absolute quantification by droplet digital PCR versus analog real-time PCR. Nat Methods 10:1003-1005.

[25] Witwer KW, McAlexander MA, Queen SE, Adams RJ (2013) Real-time quantitative PCR and droplet digital PCR for plant miRNAs in mammalian blood provide little evidence for general uptake of dietary miRNAs. RNA Biol 10:1080-1086.

[26] Shen F, Davydova EK, Du W, Kreutz JE, Piepenburg O, Ismagilov RF (2011) Digital isothermal quantification of nucleic acids via simultaneous chemical initiation of recombinase polymerase amplification reactions on SlipChip. Anal Chem 83:3533-3540.

[27] Gansen A, Herrick AM, Dimov IK, Leeb LP, Chiua DT (2012) Digital LAMP in a sample self-digitization (SD) chip. Lab Chip 12:2247-2254.

[28] Blainey PC, Quake SR (2011) Digital MDA for enumeration of total nucleic acid contamination. Nucleic Acids Research 39:e19.

[29] Konry T, Smolina I, Yarmush JM, Irimia D, Yarmush ML (2011) Ultrasensitive detection of low-abundance surface-marker protein using isothermal rolling circle amplification in a microfl uidic nanoliter platform. Small 7:395-400.

[30] Mazutis L, Araghi AF, Miller OJ, Baret JC, Frenz L, Janoshazi A, Taly V, Miller BJ, Hutchison JB, Link D, Griffiths AD, Ryckelynck M (2009) Droplet-based microfluidic systems for high-throughput single DNA molecule isothermal amplification and analysis. Anal Chem 81:4813-4821.

[31] Fasanaro P, D'Alessandra Y, Di Stefano V, Melchionna R, Romani S, Pompilio G, Capogrossi MC, Martelli F (2008) MicroRNA-210 modulates endothelial cell response to hypoxia and inhibits the receptor tyrosine kinase ligand ephrin-A3. J Biol Chem 283:15878-15883.

[32] Manicardi A, Fabbri E, Tedeschi T, Sforza S, Bianchi N, Brognara E, Gambari R, Marchelli R, Corradini R (2012) Cellular uptakes, biostabilities and anti-miR-210 activities of chiral arginine-PNAs in leukaemic K562 cells. Chem Bio Chem 13:1327-1337.

[33] Fabbri E, Manicardi A, Tedeschi T, Sforza S, Bianchi N, Brognara E, Finotti A, Breveglieri G, Borgatti M, Corradini R, Marchelli R, Gambari R (2011) Modulation of the biological activity of microRNA-210 with peptide nucleic acids (PNAs). Chem Med Chem 6:2192-2202.

[34] Whitehead CL, Teh WT, Walker SP, Leung C, Larmour L, Tong S (2013) Circulating MicroRNAs in maternal blood as potential biomarkers for fetal hypoxia in-utero. PLoS One 8:e78487.

[35] Røsjø H, Dahl MB, Bye A, Andreassen J, Jørgensen M, Wisløff U, Christensen G, Edvardsen T, Omland T (2014) Prognostic value of circulating microRNA-210 levels in patients with moderate to severe aortic stenosis. PLoS One 9:e91812.

[36] Zhao A, Li G, Péoc'h M, Genin C, Gigante M (2013) Serum miR-210 as a novel biomarker for molecular diagnosis of clear cell renal cell carcinoma. Exp Mol Pathol 94:115-20.

[37] Ho AS, Huang X, Cao H, Christman-Skieller C, Bennewith K, Le QT, Koong AC (2010) Circulating miR-210 as a Novel Hypoxia Marker in Pancreatic Cancer. Transl Oncol 3:109-13.

[38] Cheng HH, Mitchell PS, Kroh EM, Dowell AE, Chéry L, Siddiqui J, Nelson PS, Vessella RL, Knudsen BS, Chinnaiyan AM, Pienta KJ, Morrissey C, Tewari M (2013) Circulating microRNA profiling identifies a subset of metastatic prostate cancer patients with evidence of cancer-associated hypoxia. PLoS One 8:e69239.

[39] Jung EJ, Santarpia L, Kim J, Esteva FJ, Moretti E, Buzdar AU, Di Leo A, Le XF, Bast RC Jr, Park ST, Pusztai L, Calin GA (2012) Plasma microRNA 210 levels correlate with sensitivity to trastuzumab and tumor presence in breast cancer patients. Cancer 118:2603-14.

[40] D'Agata R, Corradini R, Ferretti C, Zanoli L, Gatti M, Marchelli R, Spoto G (2010) Ultrasensitive detection of non-amplified genomic DNA by nanoparticle-enhanced surface plasmon resonance imaging. Biosens Bioelectron 25:2095-2100.

[41] Grasso G; D'Agata R; Zanoli L, Spoto G (2009) Microfluidic networks for surface plasmon resonance imaging real-time kinetics experiments. Microchem J 93: 82-86.

[42] Tice JD, Lyon AD, Ismagilov RF (2004) Effects of viscosity on droplet formation and mixing inmicrofluidic channels. Anal Chim Acta 507:73-77.

[43] Yin BC, Liu YQ, Ye BC (2013) Sensitive detection of microRNA in complex biological samples via enzymatic signal amplification using DNA polymerase coupled with nicking endonuclease. Anal Chem 85:11487-93.

[44] Bi S, Zhang J, Hao S, Ding C, Zhang S (2011) Exponential amplification for chemiluminescence resonance energy transfer detection of microRNA in real samples based on a cross-catalyst strand-displacement network. Anal Chem 83:3696-702.

[45] Persat A, Chivukula RR, Mendell JT, Santiago JG (2010) Quantification of global microRNA abundance by selective isotachophoresis. Anal Chem 82, 9631-9635.

[46] Wang J, Yi X, Tang H, Han H, Wu M, Zhou F (2012) Direct quantification of microRNA at low picomolar level in sera of glioma patients using a competitive hybridization followed by amplified voltammetric detection. Anal Chem 84:6400-6406.